مجلة التربوي
Journal of Educational
ISSN: 2011- 421X
Arcif Q3

معامل التأثير العربي 1.63
العدد 22

مجلة التربوي

مجلة علمية محكمة تصدر عن

كلية التربية / الخمس

جامعة المرقب

العدد الثاني والعشرون

يناير 2023م

ضوابط النشر:

يشترط في البحوث العلمية المقدمة للنشر أن يراعى فيها ما يأتي :

-أصول البحث العلمي وقواعده .

-ألا تكون المادة العلمية قد سبق نشرها أو كانت جزءا من رسالة علمية .

-يرفق بالبحث تزكية لغوية وفق أنموذج معد .

-تعدل البحوث المقبولة وتصحح وفق ما يراه المحكمون .

-التزام الباحث بالضوابط التي وضعتها المجلة من عدد الصفحات ، ونوع الخط ورقمه ، والفترات الزمنية الممنوحة للتعديل ، وما يستجد من ضوابط تضعها المجلة مستقبلا .

تنبيهات :

-للمجلة الحق في تعديل البحث أو طلب تعديله أو رفضه .

-يخضع البحث في النشر لأولويات المجلة وسياستها .

-البحوث المنشورة تعبر عن وجهة نظر أصحابها ، ولا تعبر عن وجهة نظر المجلة .

Information for authors

1- Authors of the articles being accepted are required to respect the regulations and the rules of the scientific research.

2- The research articles or manuscripts should be original and have not been published previously. Materials that are currently being considered by another journal or are a part of scientific dissertation are requested not to be submitted.

3- The research articles should be approved by a linguistic reviewer.

4- All research articles in the journal undergo rigorous peer review based on initial editor screening.

5- All authors are requested to follow the regulations of publication in the template paper prepared by the editorial board of the journal.

Attention

1- The editor reserves the right to make any necessary changes in the papers, or request the author to do so, or reject the paper submitted.

2- The research articles undergo to the policy of the editorial board regarding the priority of publication.

3- The published articles represent only the authors' viewpoints.

مجلة التربوي
Journal of Educational
ISSN: 2011- 421X
Arcif Q3

معامل التأثير العربي 1.63
العدد 22

Rutherford backscattering spectrometry (review)

Hameda Ali Abrass
Department of Physics, Faculty of Science, Elmergib University
habrass@elmergib.edu.ly

Abstract: The paper will describe all the details about Rutherford Backscattering Spectrometry (RBS) Technique. The well-collimated beam of energetic particles is shot into a high-vacuum scattering chamber containing the target. The energy of the backscattered ions is then measured from scattering events occurring at both the surface and a particular depth. The typical backscattering angles used are optimised for mass resolution at $160° \leq \theta \leq 170°$.
Keywords: Rutherford, Backscattering, Spectrometry, Technique, Thin films.

Introduction

In Rutherford backscattering spectrometry (RBS), charged particles like He^+ or H^+ are incident on a target material. The charged particles used in this case were helium ions (He^+). The first occurrence of backscattering was carried out by Geiger and Marsden in 1909 [1], the effects of which were later explained by the Rutherford atomic model in 1911 [2]. But it was during the 1960s that RBS became an important and commonly applied technique for the study of thin films, silicide formation, and diffusion studies [3]. The technique has the advantage of allowing analysis to be done reliably and with almost no destruction [4]. RBS is a fast and direct method for obtaining element depth profiles in solids [4, 5]. The RBS technique, simple in nature, is a non-destructive analytical tool for the microanalysis of materials, and the most suitable for measuring heavy elements on light substrates [6]. The well-collimated beam of energetic particles is shot into a high-vacuum scattering chamber containing the target [7]. The energy of the backscattered ions is then measured from scattering events occurring at both the surface and a particular depth. The typical backscattering angles used are optimised for mass resolution at $160° \leq \theta \leq 170°$ [3].

When a beam of mono-energetic ions is incident a material, some of the projectile ions will be elastically scattered in two different ways, depending on the energy and velocity of the ion. The interactions occur either with the orbital electrons or the nuclei of the target atoms. The RBS technique is based on the principle that the energy of an elastically backscattered particle depends on the mass of the target atom (kinematic factor), the depth at which the scattering event takes place (energy loss into and from the point of interaction) and the scattering cross-section [8]. The RBS technique can determine the masses of the elements used and thus their chemical composition in a sample, and their depth profiles over distances as small as a few nanometres to about 2 μm for incident He^+ ions from the surface. This technique allows for the determination of crystalline structure through channelling experiments [9], [10]. The RBS technique is best suited for analysing thin films and multi-layered structures, and can determine the composition and depth profiles with a depth resolution of typically ten nanometres over a depth of hundreds of nanometres without eroding the material surface [11], [12]. The elemental composition of a sample may be determined to very good precision, since RBS is very sensitive to heavy elements in the order of parts per million. The signals between peaks can convey information about the diffusion, interface creation and phase changes. This extends the RBS technique's capabilities into the measurement of the kinetics of transformation in thin film structures.

The setup of the accelerator as illustrated in Figure 1 was capable of producing a He^+ beam with energy of 2.0 MeV, but the energies used in most of study were 1.4 and 1.6 MeV. Lower beam energy in conventional RBS has been known to extend the depth resolution and sensitivity of the RBS technique, as observed by Brijs et al. [13].

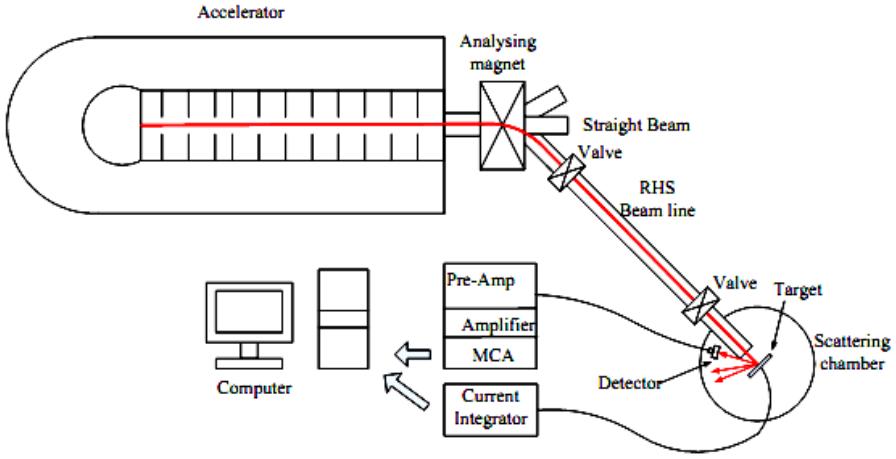

Figure1: Schematic overview of the RBS setup [14].

A beam of mono-energetic (in the MeV range) collimated He^+ particles impinge on a target and a fraction of the backscattered particles is analysed with a silicon barrier detector placed at a fixed scattering angle. The scattered particles that strike the detector generate an electrical signal proportional to their energy, which is amplified and processed with rapid analogue and digital electronics. The data collected in the final stage has the form of a digitised spectrum [15]. The backscattering energy spectra of counts against channel number were obtained by collecting a charge of $8\mu c$, constituting a run.

RBS essentially relies on the following three physical concepts:

- The kinematic factor *K*,
- The energy loss of a particle $(\frac{dE}{dx})$, and
- The differential scattering cross-section $(\frac{d\sigma}{d\Omega})$.

Kinematic factor

When a beam of He^+ particles collides with a stationary target atom the incident particles may be scattered by the target atoms. Provided that the energy of the incident particles is considerably larger than the binding energy of atoms in the target, but also below the energy at which nuclear reactions will occur, the interaction can be treated as a simple elastic collision Figure 2 illustrates, a collision between an incident energetic particle with mass M_1, velocity υ_o, energy E_o and a target atom with mass M_2. During the collision, a transfer of energy from the moving particle to the stationary target atom occurs, leading to final velocities and energies υ_1, E_1 and υ_2, E_2 respectively.

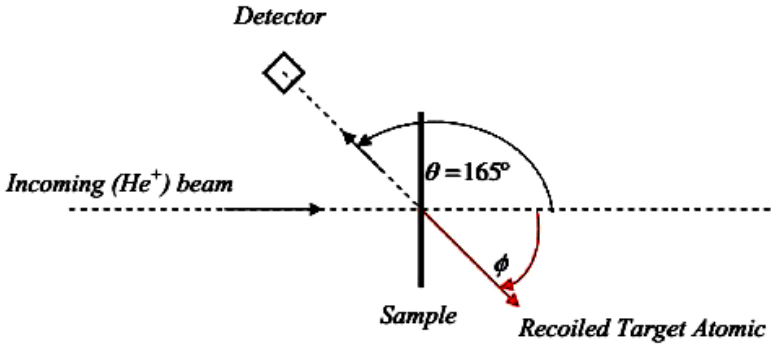

Figure2: Schematic diagram showing the RBS experimental setup at the University of Pretoria [16].

The reduction in energy of the scattered incident particles depends on the masses of the incident and target atoms. The ratio of the projectile energies, E_o and E_l,are defined as kinematic factor *K*.

$$K = \frac{E_1}{E_o} \qquad (1)$$

If the collision between the incident particle (He^+ particles) M_1 and the stationary target particle of mass M_2, as shownin the equation below, is an elastic collision, it can be described. Based on this decription, the energy of the backscattered incident He^+ particle is given as[15]:

$$E_1 = KE_o = \left[\frac{M_1 cos\theta \pm \left(M_2^2 - M_1^2 sin^2\theta\right)^{1/2}}{M_1 + M_2}\right]^2 E_o \qquad (2)$$

E_o and E_1 are respectively the incident and backscattered energies of the alpha particles. The energy ratio of the incident particle before and after collision is the kinematic factor *K* and θ is the backscattering angle. Equation (2) must be adapted if the incident particle travels deeper into the substrate material. From the above equation it is clear that the energy of the backscattered He^+ particle E_1can be calculated if the kinematic factor *K* is known. *K* can be calculated using M_1, M_2 and the scattering angle θ. At a fixed scattering angle, the kinematic factor *K* depends only on the mass ratio, namely M_1/M_2. The plus sign in equation (2) is only valid when $M_1 < M_2$, but when $M_1 > M_2$ there are two solutions, resulting in two kinematic factors *K* for backscattered He^+ particles at angle θ corresponding to different recoil angles [15]. Then incident He^+ particles of the same energy and incident angle will have varying backscattered energies when they bombard target particles that have different masses,which justifies the use ofthe use of Rutherford backscattering to identify the constituents of a sample. Equation (2) shows the dependence of the backscattered particle's energy on the target mass and the scattering angle θ. However, during measurement the kinematic factor *K* only depends on the mass of the target atom M_2, since the detector angle θ and the mass of the projectile M_1 is constant. If the energy of the projectile E_o and its mass M_1 are known, one can determine M_2 (i.e. the mass of the atoms from which they are scattered), by measuring the energy E_1 of the backscattered particles. It is also evident from equation (2) that the energy of the particles scattered by the heaviest element is higher than those scattered by lighter ones.

Furthermore, the energy E_1 of the projectile attains its maximum value when the scattering angle θ is 180º. The importance of the kinematic factor is that it describes the reduction of incident energy during the collision, and this then allows identification of the target atom's mass by measuring the scattered particle's energy.

Depth scaling of thin film systems

With regard to thin films deposited on the substrates, it is mainly the stoichiometry and depth profile of heavy elements within that are of primary interest here.

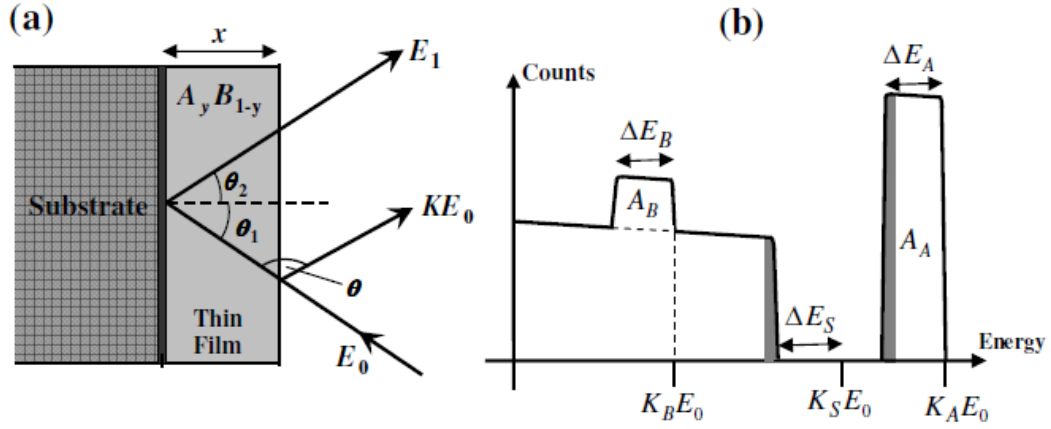

Figure 3: (a) Scattering geometry and (b) spectrum of an RBS measurement of a thin compound target.

Figure 3 shows the scattering layout and the RBS spectrum of a thin compound film A_yB_{1-y} on a substrate *S*, where in many cases during semiconductor research, *A* is usually a heavy element, *B* is either *O* or *N*, and *S*is usually Si. The signals from elements *A* and *B* in the spectrum have high energy edges at K_AE_0 and K_BE_0 respectively, with the substrate signal *S* pushed back to lower energy by ΔE_s due to the ions losing energy within the thin film. The signal from *B* rests on top of the substrate signal *S*, due to $K_BE_0 < K_sE_0 - \Delta E_s$. Elemental depth profiling of the thin film is shown more clearly in the signal from *A*, which is isolated at higher energies.

Collisions with atoms of both *A* and *B* will now contribute to the energy loss process. Ions will lose the same amount of energy per unit length along the way in, but may lose a different amount along the way out, depending from which atom they backscatter, due to the difference in *K* values. The energy widths of the respective signals in the spectrum are:

$$\Delta E_A = [S]_A^{AB} N^{AB} x \text{ and } \Delta E_B = [S]_B^{AB} N^{AB} x \qquad (3)$$

with

$$[S]_A^{AB} = \frac{K_A}{\cos\theta_1} S_{IN}^{AB} + \frac{1}{\cos\theta_2} S_{OUT.A}^{AB} \qquad (4)$$

$$[S]_B^{AB} = \frac{K_B}{\cos\theta_1} S_{IN}^{AB} + \frac{1}{\cos\theta_2} S_{OUT.B}^{AB} \quad (5)$$

and where $N^{AB}x$ is the areal density of the thin film, S_{IN}^{AB} is the stopping cross-section of the ions along the way in, while $S_{OUT.A}^{AB}$ and $S_{OUT.B}^{AB}$ are the cross-sections along the way out after backscattering from atoms of *A* and *B* respectively. We assume that Bragg's rule of additivity applies to the stopping cross-sections for both inward and outward paths at the same energy *E*, so that:

$$S^{AB}(E) = [y]S_A(E) + [1-y]S_B(E) \quad (6)$$

The area of the signals in the spectrum from elements *A* and *B* are:

$$A_A = \frac{\Omega}{\cos\theta_1} \int_{E_0}^{E_x} \frac{\sigma_A(E)}{S_A(E)} dE \quad (7)$$

and

$$A_B = \frac{\Omega}{\cos\theta_1} \int_{E_0}^{E_x} \frac{\sigma_B(E)}{S_B(E)} dE \quad (8)$$

These can then be used to determine the stoichiometric ratio between the elements in the film. Depth profiles of elements *A* and *S* are shown in shaded regions in the spectrum.

Energy loss

When the alpha particle penetrates a target, it loses energy along its trajectory due to interaction between bound and free electrons, and to small-angle nuclear collisions, which is only of significance at low energies. The magnitude of energy lost depends on the total distance travelled by the incident particles, and on the density and composition of the target, as well as the incident particle's velocity [17]. The energy loss per unit length dE/dx at the energy *E* of the incident projectile is defined as:

$$\lim_{\Delta x \to 0} \frac{\Delta E}{\Delta x} \equiv \frac{dE}{dx}(E) \quad (9)$$

Depth scaling explains the relationship between the exit (from the substrate) energy $E_1$of the alpha particle, backscattered at depth *x* inside the target substrate (see Figure 4. The energy of the incident alpha particle in the equation below is given as E_o. The energy E_o reduces to *E* just before the backscattering because the particle loses energy as it moves through the substrate. The backscattered particle at depth *x* loses more energy while exiting the target and eventually reduces to the exit energy E_1.

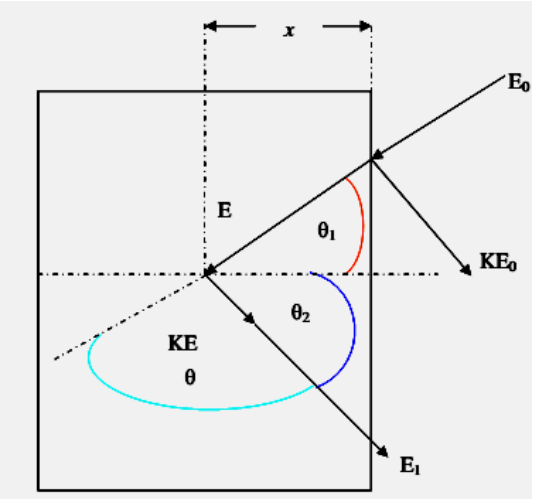

Figure 4: A schematic diagram showing the backscattering events in a target consisting of one element. The angles θ_1 and θ_2 are positive regardless of the side on which they lie with respect to the normal of the target [16].

The energy lost by the alpha particle upon entering the target particle is given as $E_o - E$, while the energy lost on its way out is given as $KE_o - E_1$. Assuming that the energy loss $(dE|dx)$ is constant over each path, the energy of the backscattered alpha particle at depth x is then given as [15, 18]:

$$KE_o - E_1 = \left[\frac{K}{cos\theta_1}\frac{dE}{dx}(in) + \frac{1}{cos\theta_2}\frac{dE}{dx}(out)\right]x \qquad (10)$$

The subscripts 'in' and 'out' refer to the constant values along the inward and outward paths. KE_o is the energy of the backscattered particles scattered from surface atoms of the target particle.

If ΔE is the energy difference between $E_1$and KE_o, then:

$$\Delta E = KE_o - E_1 \qquad (11)$$

The term$\frac{K}{cos\theta_1}\frac{dE}{dx}(in) + \frac{1}{cos\theta_2}\frac{dE}{dx}(out)$ in equation (10) above is the backscattering energy-loss factor [S]. It gives the relationship between the backscattered energy and the depth. Equation (10) can be rewritten as:

$$\Delta E = [S]x \qquad (12)$$

Scattering cross-section

The scattering cross-section provides the relationship between the number of target atoms and detected particles. The number of particles that will be identified in a detector with solid angle Ω is determined by:

$$Y = \sigma(\theta)\Omega Q N_s \qquad (13)$$

In such a case where $\sigma(\theta)$ is the scattering cross-section, a particle is backscattered towards a detector at an angle θ, Ns being the number of target atoms per cm^2 and Q the total number of incident particles [15, 17]. By considering the Coulomb repulsion of two nuclei (which is the case with RBS energy), the differential scattering cross-section can be calculated [15] with the Rutherford scattering cross-section in the laboratory frame of reference,

$$\frac{d\sigma}{d\Omega} = \left[\frac{Z_1 Z_2 e^2}{2E}\right]^2 \frac{\left[cos\theta + (1 - M_1/M_2\, sin^2\theta)^{1/2}\right]^2}{sin^4\,\theta\,(1 - M_1/M_2\, sin^2\theta)^{1/2}} \qquad (14)$$

where Z_1 and Z_2 are the respective atomic numbers of the projectile particles of mass M_1 and target atoms of mass M_2. It is clear from equation (14), that the differential cross-section $\sigma(\theta)$ depends on Z_2^2, which indicates that RBS is significantly more sensitive to high Z elements. Therefore, if equal amounts of a light and heavy element are present, the number of particles scattered from the heavy element will be much greater.

RBS analysis

RBS analysis was performed to obtain the elemental composition of the sample, the thickness of deposited Co film and the thickness of the reaction area. The RBS spectrum of the sample is shown in Figure 5, along with the simulated spectra done using the Rutherford Universal Manipulation Program (RUMP) computer code [19].

The black line indicates the raw RBS data and the red line is the simulation line. RBS analysis using RUMP found the Co layer to be 1130×10^{15} at/cm^2 thick. Assuming an atomic density of 9.00×10^{22} at/cm^3, this yields a thickness of 126 nm. This is of course a lower bound on the Co thickness, as the actual density of the layer may well be less than the standard density. The vertical axis is the normalised yield; that is, the number of particles scattered into the detector and normalized to the total incident beam dosage, the detector solid angle, and the channel width of the multichannel analyser [20].

This normalisation procedure allows direct comparison of spectra from the different samples. The energy of the backscattered particles and channel numbers are plotted on the horizontal axis of this graph. The arrows in the graph shown in Figure 5 indicate the surface positions of Si and Co.The peak observed at about 1.15 MeV is from the enriched Zr part of the FeZr layer and is superimposed on the Co-signal.

The corresponding Fe signal is visible between channels 300-340. The narrowness of the Zr peak is due to the overgrowth of a thin Zr layer. Due to the asymmetric e-gun geometry the rest of the Zr peak overlaps with Co, up to energy of 1.08 MeV. The FeZr was found to be 490×10^{15} at/cm^2 thick. Assuming that the density of FeZr can be estimated from the elemental densities, this equals 63 nm.

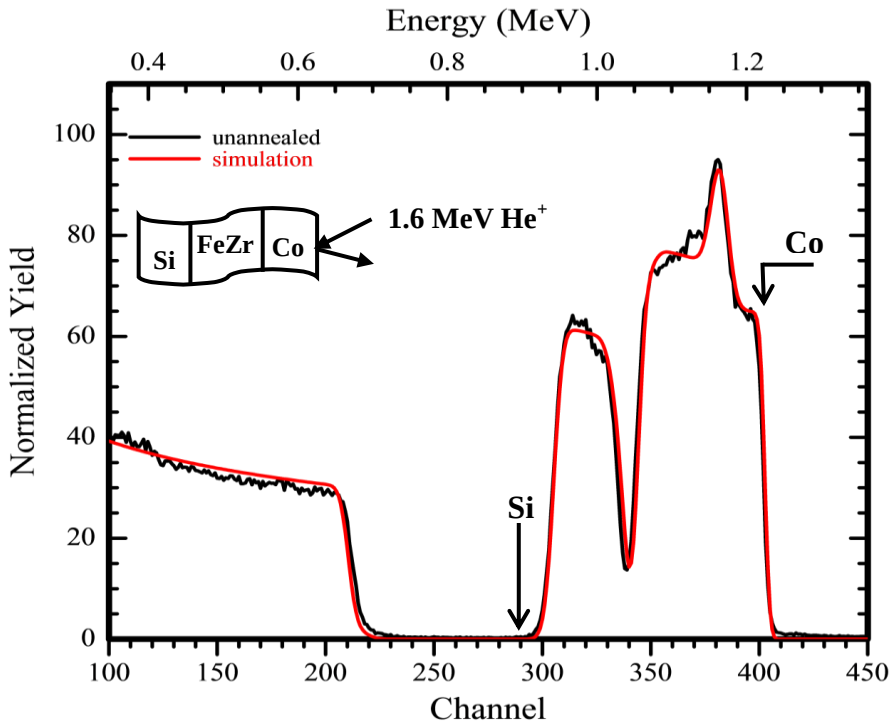

Figure 5:Raw RBS spectrum of Si/FeZr/Co sample with RUMP simulation spectrum.

Conclusion

Through this detailed study on RBS technique. It is clear to us that this technique became an important and commonly applied technique that used until now tostudy of thin films, silicide formation, and diffusion studies. The technique has the advantage of allowing analysis to be done reliably and with almost no destruction. RBS is a fast and direct method for obtaining element depth profiles in solids. The RBS technique, simple in nature, is a non-destructive analytical tool for the microanalysis of materials, and the most suitable for measuring heavy elements on light substrates.

References

1. H. Geiger and E. Marsden, "On a diffuse reflection of a particles", *Royal Society 82, (1909) 495-500.*
2. E. Rutherford, "The scattering of Q: and (3) particles by matter and the structure of the atom", *Philosophical Magazine 21, (1911) 669-688.*
3. W. K. Chu, J. W. Mayer, M. A. Nicolet, T. M. Buck, G. Amsel, and F. Eisen, “Principles and applications of ion beam techniques for the analysis of solids and thin films,” Thin Solid Films, vol. 17, pp. 1–41, 1973.
4. J. F. Ziegler, "Material analysis by nuclear backscattering", *Prenum press, New York, (1975).*
5. W. K. Chu, J. W. Mayer, M. A. Nicolet, T. M. Buck, G. Amsel, and F. Eisen, "Principles and applications of ion beam techniques for the analysis of solids and thin films", *Thin solid films, 17, (1973) 1-41.*

6. K. Kusao, M. Satoh, and K. Morita, “An Area Ratio Method for RBS Compositional Analysis of Thin films,” Surface and Interface Analysis, vol. 18, pp. 417–420, 1992.
7. H. Matzke, “Application of Ion Beam Techniques to Solid State Physics and Technology of Nuclear Materials,” Journal of Nuclear Materials, vol. 136, pp. 143–153, 1985.
8. L. G. Earwaker, “Rutherford backscattering and nuclear reaction analysis,” Vacuum, vol. 45, pp. 783–803, 1994.
9. C. Jeynes, Z. H. Jafri, R. P. Webb, A. C. Kimber, and M. J. Ashwin, “Accurate RBS Measurements of the Indium Content of InGaAs Thin Films,” Surface and Interface Analysis, vol. 25, pp. 254–260, 1997.
10. P. Aloupogiannis, A. Travlos, X. Aslanoglou, M. Pilakouta, and G. Weber, “Rare-earth silicide thin film study. Comparison of heavy ion and conventional RBS,” Vacuum, vol. 44, pp. 37–39, 1993.
11. A. Climent-Font, M. T. Fernandez-Jimenez, U. Watjen, and J. Perriere, “RBS: An analytical technique for elemental characterization of standards; advantages and limits of application,” Nuclear Instruments and Methods in Physics Research A, vol. 353, pp. 575–578, 1994.
12. L. Palmetshofer, “Surface and Thin Film Analysis,” in Surface and Thin-film Analysis, H. Bubert and G. Friedbacher, Eds. Weinheim: Wiley Online Library, 2011, pp. 191–202.
13. B. Brijs, J. Deleu, C. Huyghebaert, S. Nauwelaerts, K. Nakajima, K. Kimura, and W. Vander vorst, "Advanced RBS Analysis of Thin Films in Micro-Electronics", *in Application of Accelerators in Research and Industry - Sixteenth International Conference, 3, (2001)470–475.*
14. J. Brahamcha, "Physique-Nanoscience 2nd Year, Production of CuZr alloys with fixed stoichiometry and different microstructures (amorphous or nanocrystalline)", 2013.
15. W. K. Chu, J. W. Mayer and M. A. Nicolet, "Backscattering spectrometry", *Academic Press, New York, (1978).*
16. T. T. Hlatshwayo, Diffusion of Silver in 6H-SiC, *University of Pretoria, 2010.*
17. L. C. Feldman and L. W Mayer, "Fundamentals of surface and thin film analysis, *North Holland, New York, (1986).*
18. J. R. Tesmer, M. A. Nastasi, J. C. Barbour, C. J. Maggiore, J. W. Mayer, "Handbook of Modern Ion Beam Materials Analysis", *Materials Research Society, Pittsburgh, PA, 1995.*
19. L. R. Doolittle, "Algorithms for the rapid simulation of Rutherford backscattering spectra.", *Nuclear Instruments and Methods in Physics Research Section B: Beam Interactions with Materials and Atoms., 9.3, (1985) 344-351.*
20. T. Wu and D. L. Kohlstedt, “Rutherford Backscattering Spectroscopy Study of the Kinetics of Oxidation of $(Mg,Fe)_2SiO4$,” Journal of American Ceramic Society, vol. 45, pp. 540–545, 1988.

مجلة التربوي
Journal of Educational
ISSN: 2011- 421X
Arcif Q3

معامل التأثير العربي 1.63
العدد 22

الفهـــــــــرس